

Electron-impact ionization in the magnesium-isoelectronic sequence

M. S. Pindzola,* D. C. Griffin,† and C. Bottcher

Physics Division, Oak Ridge National Laboratory, Oak Ridge, Tennessee 37831

(Received 2 December 1985)

Excitation-autoionization contributions to the electron-impact ionization of the Mg-like ions S^{4+} , Cl^{5+} , and Ar^{6+} are calculated in the distorted-wave approximation. The calculations indicate that the largest contributions are due to the $2p \rightarrow 3p$ monopole and $2p \rightarrow 3d$ dipole excitations from either the $2p^6 3s^2$ ground-state configuration or the $2p^6 3s 3p$ excited-state configuration. Excellent agreement with the experimental crossed-beam measurements of Howald *et al.* is obtained when one assumes that a substantial fraction of the ions coming from the electron cyclotron resonance ion source are in metastable states of the $2p^6 3s 3p$ excited-state configuration.

Experimental checks¹ on the vast body of theoretical work² concerning electron-impact excitation of atomic ions are quite limited. Some insight into the validity of excitation theory can, however, be made by comparison with the more numerous crossed-beam ionization studies of features identified as excitation followed by autoionization.³ The present theoretical study focuses on the contributions of excitation-autoionization to the electron-impact ionization of several multiply charged ions in the magnesium-isoelectronic sequence. As will be shown later the largest contributions are due to $2p \rightarrow 3p$ monopole and $2p \rightarrow 3d$ dipole excitations which are of current interest in short-wavelength laser research.⁴ The recent experimental crossed-beam measurements of Howald *et al.*⁵ for S^{4+} , Cl^{5+} , and Ar^{6+} show a clean separation between sizable excitation-autoionization features and the background direct-ionization process at incident electron energies around twice the ionization threshold. The measurements present a clear challenge to theoretical interpretation and calculation.

Electron-impact ionization of an atomic ion labeled A can follow two paths:

$$e^- + A^{n+} \rightarrow A^{(n+1)+} + e^- + e^-, \tag{1}$$

or

$$e^- + A^{n+} \rightarrow (A^{n+})^* + e^- \rightarrow (A^{(n+1)+} + e^-) + e^-. \tag{2}$$

The first process is direct ionization while the second is excitation-autoionization. It is assumed that these pro-

cesses are independent and that radiative stabilization of the autoionization states is negligible for low stages of ionization along the Mg-isoelectronic sequence. This latter assumption was tested by explicit calculation of branching ratios for several of the doubly excited configurations considered in this paper.

The electron-impact direct-ionization cross section for Ar^{6+} has been calculated in the average-configuration distorted-wave approximation.⁶ Using the experimental ionization potentials for the outer shell,⁷ we scaled the Ar^{6+} results to obtain direct-ionization cross sections for S^{4+} and Cl^{5+} .

The electron-impact excitation cross section to autoionizing levels may also be calculated in the average-configuration distorted-wave approximation. The most general transition between configurations is of the form

$$(n_1 l_1)^{q_1} (n_2 l_2)^{q_2} k_i l_i \rightarrow (n_1 l_1)^{q_1 - 1} (n_2 l_2)^{q_2 + 1} k_f l_f, \tag{3}$$

where n_i is the principal quantum number, l_i is the angular-momentum quantum number, q_i is the occupation number, and k_i is the linear-momentum wave number. The average-configuration excitation cross section (in atomic units) is given by

$$\sigma_{exc} = 8\pi q_1 \frac{(4l_2 + 2 - q_3)}{k_i^3 k_f} \times \sum_{l_i, l_f} (2l_i + 1)(2l_f + 1) M(2f; 1i), \tag{4}$$

where

$$\begin{aligned} M(2f; 1i) = & \sum_{\lambda} \begin{bmatrix} l_1 & \lambda & l_2 \\ 0 & 0 & 0 \end{bmatrix}^2 \begin{bmatrix} l_i & \lambda & l_f \\ 0 & 0 & 0 \end{bmatrix}^2 \frac{[R^{\lambda}(2f; 1i)]^2}{(2\lambda + 1)} \\ & + \sum_{\lambda'} \begin{bmatrix} l_1 & \lambda' & l_f \\ 0 & 0 & 0 \end{bmatrix}^2 \begin{bmatrix} l_i & \lambda' & l_2 \\ 0 & 0 & 0 \end{bmatrix}^2 \frac{[R^{\lambda'}(f2; 1i)]^2}{(2\lambda' + 1)} \\ & - \sum_{\lambda, \lambda'} (-1)^{\lambda + \lambda'} \begin{bmatrix} l_1 & l_2 & \lambda \\ l_i & l_f & \lambda' \end{bmatrix} \begin{bmatrix} l_1 & \lambda & l_2 \\ 0 & 0 & 0 \end{bmatrix} \begin{bmatrix} l_i & \lambda & l_f \\ 0 & 0 & 0 \end{bmatrix} \begin{bmatrix} l_1 & \lambda' & l_f \\ 0 & 0 & 0 \end{bmatrix} \begin{bmatrix} l_i & \lambda' & l_2 \\ 0 & 0 & 0 \end{bmatrix} R^{\lambda}(2f; 1i) R^{\lambda'}(f2; 1i). \end{aligned} \tag{5}$$

TABLE I. Average-configuration excitation cross sections from the $2p^63s^2$ ground-state configuration.

Ion	Configuration transition	Average excitation energy (eV)	Cross section (10^{-18} cm 2) at threshold energy	Cross section (10^{-18} cm 2) at twice threshold energy
S^{4+}	$2p^63s^2 \rightarrow 2p^53s^23p$	171.3	1.43	0.683
	$2p^53s^23d$	191.2	1.47	0.906
	$2p^53s^24p$	207.2	0.257	0.115
	$2p^53s^24d$	213.2	0.417	0.248
Cl^{5+}	$2p^63s^2 \rightarrow 2p^53s^23p$	210.9	1.04	0.489
	$2p^53s^23d$	234.2	1.23	0.771
	$2p^53s^24p$	258.2	0.190	0.084
	$2p^53s^24d$	265.4	0.335	0.199
Ar^{6+}	$2p^63s^2 \rightarrow 2p^53s^23p$	254.3	0.764	0.358
	$2p^53s^23d$	281.0	1.01	0.639
	$2p^53s^24p$	314.3	0.141	0.061
	$2p^53s^24d$	322.7	0.264	0.157

In Eq. (5), $R^\lambda(ij;rt)$ is the usual Slater radial integral for the Coulomb interaction between electrons and the continuum normalization is chosen as one times a sine function. The bound-state energies and atomic orbitals needed to evaluate Eq. (4) are generated using the radial wavefunction code developed by Cowan.⁸ The continuum radial orbitals, or distorted waves, are calculated using a local semiclassical approximation for the exchange interaction.⁹

Average-configuration excitation cross-section results for S^{4+} , Cl^{5+} , and Ar^{6+} are given in Table I. The average excitation energies are in good agreement with the onset of experimental excitation-autoionization features.⁵ The largest contributions come from the $2p \rightarrow 3p$ monopole and $2p \rightarrow 3d$ dipole excitations.

In order to take into account the energy-level spread within each configuration, we have adopted a simple procedure called the average-statistical model (ASM). The average-configuration collision cross section for either the direct-ionization or excitation-autoionization process is statistically partitioned over all levels of the final ionized

or excited configuration. The total cross section is then summed taking explicit account of the energy position of each level calculated using an atomic-structure program provided by Cowan.⁸

In Fig. 1, ASM calculations for S^{4+} in the threshold energy region are compared with a more detailed intermediate-coupled level-to-level distorted-wave calculation. The level-to-level calculation has been described previously in work on the transition-metal ions.¹⁰ As shown in Fig. 1 the 10 levels of the $2p^53s^23p$ configuration are spread over 10.3 eV starting at 169.1 eV, while the 12 levels of $2p^53s^23d$ configuration have a spread of 3.9 eV starting at 189.8 eV. The major discrepancy between the two calculations is for the $2p^53s^23p^1S_0$ level at 179.4 eV for which the level-to-level method attributes over half the total configuration cross section, even though its statistical weight is quite small. On the other hand the total collision cross sections from each of the two calculations are in excellent agreement.

In Figs. 2–4, ASM calculations for S^{4+} , Cl^{5+} , and Ar^{6+} are compared with experimental crossed-beam measurements of Howald *et al.*⁵ over a wide energy range.

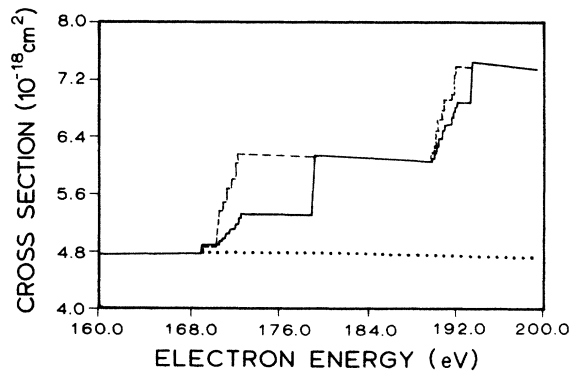


FIG. 1. Electron-impact ionization of S^{4+} near the threshold for excitation-autoionization. Solid curve, level-to-level excitation cross section plus direct cross section calculated in the distorted-wave approximation; dashed curve, total cross section in the average-statistical model; dotted curve, direct cross section only.

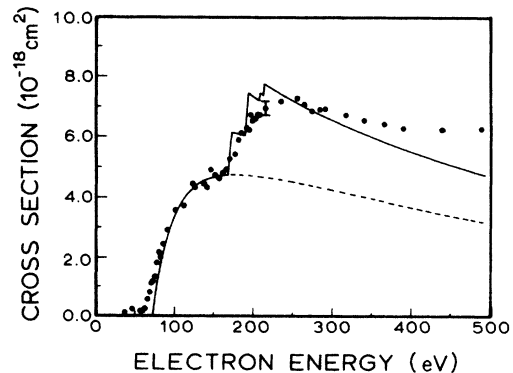


FIG. 2. Electron-impact ionization of S^{4+} . Solid curve, total cross section from the $2p^63s^2$ ground-state configuration in the average-statistical model; dashed curve, direct cross section only; solid circles, experimental measurements (Ref. 5).

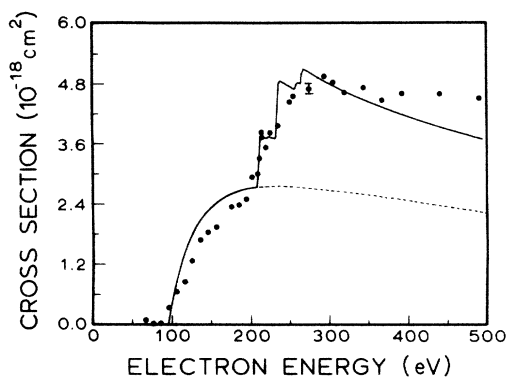


FIG. 3. Electron-impact ionization of Cl^{5+} . Solid curve, total cross section from the $2p^6 3s^2$ ground-state configuration in the average-statistical model; dashed curve, direct cross section only; solid circles, experimental measurements (Ref. 5).

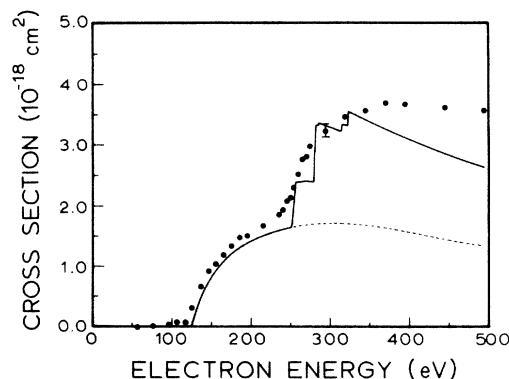


FIG. 4. Electron-impact ionization of Ar^{6+} . Solid curve, total cross section from the $2p^6 3s^2$ ground-state configuration in the average-statistical model; dashed curve, direct cross section only; solid circles, experimental measurements (Ref. 5).

Although the overall agreement between theory and experiment for the three atomic ions is quite good, there are several noteworthy discrepancies. In examining Fig. 2 for S^{4+} , we first note that the experimental direct-ionization threshold is about 10 eV lower than theory. The theoretical calculations use the spectroscopic value of 72.68 eV.⁷ We next note that the experimental excitation-autoionization features between 170 and 220 eV appear to be spread over a wider energy interval than predicted by theory. Finally, the most obvious discrepancy is the growing divergence between experiment and theory beginning at 240 eV and extending to the highest energies. Although the $2p$ -shell direct-ionization threshold is calculated to be at 236.5 eV, the branching ratio for the decay of the $2p^5 3s^2$ configuration to the $2p^6$ configuration of S^{4+} is almost 1. The same three discrepancies found in S^{4+} are found to a varying degree in Figs. 3 and 4 for Cl^{5+} and Ar^{6+} , respectively.

To help resolve the discrepancies the ASM calculations for the three Mg-like ions were repeated for electron-impact ionization from the $2p^6 3s 3p$ excited-state configuration. Of the 12 states in the $2p^6 3s 3p$ configuration, six are forbidden to decay by J selection rules. The ratio of extremely metastable excited states (millisecond lifetimes or longer) in the $2p^6 3s 3p$ excited-state configuration to all states of the ground and excited configurations is 0.46. Thus a substantial fraction of the $2p^6 3s 3p$ states may live longer than the ion-beam transit time from source to

scattering chamber in the crossed-beam experiment.⁵ Average-configuration excitation cross section results for S^{4+} are given in Table II. The active orbitals involved in excitation from the metastable state are the same as for the ground state. Hence the average excitation energies and cross sections for S^{4+} from the $2p^6 3s 3p$ excited-state configuration are about the same as those found in Table I for S^{4+} from the $2p^6 3s^2$ ground-state configuration. The same result is true for Cl^{5+} and Ar^{6+} .

In Figs. 5–7, ASM calculations for S^{4+} , Cl^{5+} , and Ar^{6+} for ionization from the $2p^6 3s 3p$ excited-state configuration are compared with the experimental measurements.⁵ In examining Fig. 5 for S^{4+} , experiment and theory are in good agreement at the direct-ionization threshold since the $2p^6 3s 3p$ excited-state configuration is on the average 10.8 eV above the $2p^6 3s^2$ ground-state configuration. We note that the $2p^6 3s 3p$ configuration has four levels spread over 7.3 eV. The $2p^5 3s 3p^2$ and $2p^5 3s 3p 3d$ autoionizing configurations have 172 levels compared to the 22 levels found previously for the $2p^5 3s^2 3p$ and $2p^5 3s^2 3d$ configurations. Hence the theoretical curve between 170 and 220 eV appears to have been smoothed out, in better agreement with experiment.

Theory and experiment for S^{4+} are in better agreement at high energies as shown by Fig. 5, since the contributions of the direct ionization out of the $2p$ subshell beginning at 238.3 eV are now included. In pure LS coupling, the states of the $2p^5 3s 3p$ configuration^{11,12} from the ^4S ,

TABLE II. Average-configuration excitation cross sections from the $2p^6 3s 3p$ excited-state configuration.

Ion	Configuration transition	Average excitation energy (eV)	Cross section (10^{-18} cm^2) at threshold energy	Cross section (10^{-18} cm^2) at twice threshold energy
S^{4+}	$2p^6 3s 3p \rightarrow 2p^5 3s 3p^2$	173.0	1.17	0.559
	$2p^5 3s 3p 3d$	191.5	1.48	0.916
	$2p^5 3s 3p 4p$	207.9	0.253	0.113
	$2p^5 3s 3p 4d$	213.9	0.414	0.246

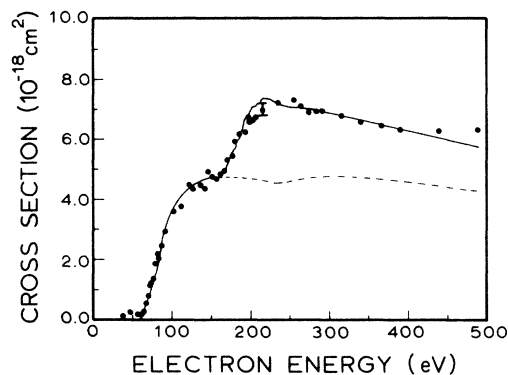


FIG. 5. Electron-impact ionization of S^{4+} . Solid curve, total cross section from the $2p^6 3s 3p$ excited-state configuration in the average-statistical model; dashed curve, direct cross section only; solid circles, experimental measurements (Ref. 5).

4P , and 4D terms of the $2p^5 3s(^3P)$ parent can neither make a dipole-allowed radiative transition nor autoionize; furthermore, the states from the 2P terms of the $2p^5 3s(^1P)$ and $2p^5 3s(^3P)$ parents cannot autoionize. Thus one might expect the states from the 2P terms to radiate to $2p^6 3p^2 P$ and the states from the quartet terms to live longer than the ion-beam transit time from the scattering chamber to the detector in the crossed-beam experiment.⁵ From this perspective only the states from the 2S and 2D terms of the $2p^5 3s(^1P)$ and $2p^5 3s(^3P)$ parents would autoionize to S^{6+} during the experiment. Since the quartet terms and the 2P terms constitute $\frac{2}{3}$ of the states of the $2p^5 3s 3p$ configuration, one can estimate that there is a $\frac{2}{3}$ probability that ionization out of the $2p$ subshell will contribute to the single-ionization cross section.

When a detailed intermediate-coupling calculation is performed on the $2p^5 3s 3p$ configuration of S^{5+} , one finds that the spin-orbit interaction causes significant mixing between the LS terms, and with the exception of states from $2p^5 3s(^3P) 3p^4 D_{7/2}$, all states should either autoionize or radiate much faster than the ion-beam transit time.

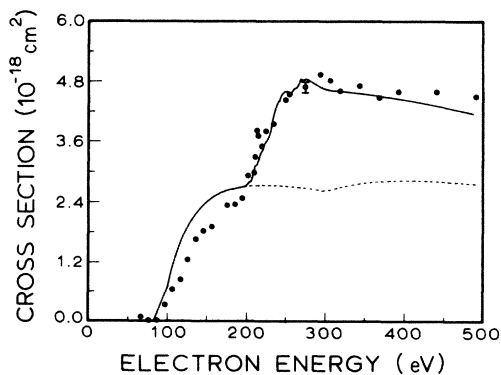


FIG. 6. Electron-impact ionization of Cl^{5+} . Solid curve, total cross section from the $2p^6 3s 3p$ excited-state configuration in the average-statistical model; dashed curve, direct cross section only; solid circles, experimental measurements (Ref. 5).

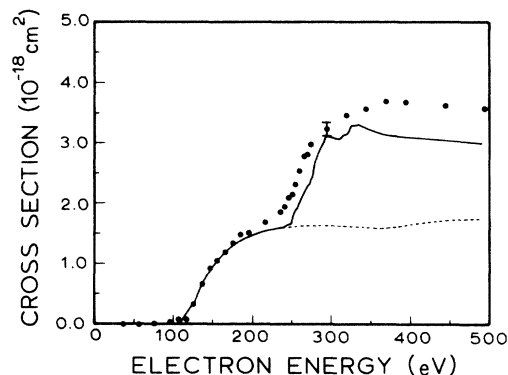


FIG. 7. Electron-impact ionization of Ar^{6+} . Solid curve, total cross section from the $2p^6 3s 3p$ excited-state configuration in the average-statistical model; dashed curve, direct cross section only; solid circles, experimental measurements (Ref. 5).

The average branching ratio for autoionization is about $\frac{1}{2}$. However, its value is quite sensitive to the exact amount of mixing and therefore somewhat uncertain. In light of these uncertainties we estimate the contribution of the $2p$ subshell to the single ionization cross section by using $\frac{2}{3}$ of the Lotz formula.¹³

The overall agreement between experiment and theory similarly improves for Cl^{5+} and Ar^{6+} as shown by Figs. 6 and 7. Part of the remaining high-energy discrepancy found in Fig. 7 for Ar^{6+} can be attributed to the obvious underestimation of the direct process by the average-configuration distorted-wave approximation.

In conclusion, the results of an ASM calculation for the electron-impact ionization of S^{4+} , Cl^{5+} , and Ar^{6+} are in quite good agreement with experimental crossed-beam measurements when one recognizes that the ion beam contains significant amounts of metastable states from the $2p^6 3s 3p$ excited configuration. From the apparent agreement, one may conclude that the theoretical prediction of the overall strength of the $2p \rightarrow 3p$ monopole and $2p \rightarrow 3d$ dipole excitations is quantitatively correct. An experimental check of the detailed level distribution of the collision cross section as found in Fig. 1, which may change when configuration-interaction and close-coupling effects are included, is not possible without a precise determination of the metastable fraction in the ion beam. However, it appears that with new generation devices such as the electron cyclotron resonance ion source, many novel atomic processes involving metastable targets will be opened up to experimental investigation.

ACKNOWLEDGMENTS

We wish to thank R. D. Cowan for making his atomic-structure program available to us and to acknowledge A. M. Howald, D. C. Gregory, and R. A. Phaneuf for a number of useful conversations concerning the ORNL-JILA experiment. We also acknowledge financial support from the Office of Fusion Energy, U.S. Department of Energy, under Contract No. DE-AC05-84OR21400 with Martin Marietta Energy Systems, Inc.

*Permanent address: Department of Physics, Auburn University, Auburn, AL 36849.

†Permanent address: Department of Physics, Rollins College, Winter Park, FL 32789.

¹D. H. Crandall, in *The Physics of Ion-Ion and Electron-Ion Collisions*, edited by F. Brouillard and J. Wm. McGowan (Plenum, New York, 1983), p. 201.

²R. J. W. Henry, *Phys. Rep.* **68**, 1 (1981).

³E. Salzborn, in *The Physics of Ion-Ion and Electron-Ion Collisions*, edited by F. Brouillard and J. Wm. McGowan (Plenum, New York, 1983), p. 239.

⁴P. Hagelstein, in *Atomic Physics 9*, edited by R. S. Van Dyck, Jr. and E. N. Fortson (World Scientific, Singapore, 1984).

⁵A. M. Howald, D. C. Gregory, F. W. Meyer, R. A. Phaneuf, A. Müller, N. Djuric, and G. H. Dunn, preceding paper, *Phys. Rev. A* **33**, 3779 (1986).

⁶S. M. Younger, *Atomic Data for Fusion*, Vol. 7, p. 190 (1981), Controlled Fusion Atomic Data Center Newsletter, Oak Ridge National Laboratory (unpublished).

⁷C. E. Moore, *Atomic Energy Levels*, Natl. Bur. Stand. Ref. Data Ser., Natl. Bur. Stand. (U.S.) Circ. No. 34 (U.S. GPO, Washington, D.C., 1970).

⁸R. D. Cowan, *The Theory of Atomic Structure and Spectra* (California Press, Berkeley, 1981).

⁹M. E. Riley and D. G. Truhlar, *J. Chem. Phys.* **63**, 2182 (1975).

¹⁰C. Bottcher, D. C. Griffin, and M. S. Pindzola, *J. Phys. B* **16**, L65 (1983).

¹¹D. C. Griffin, C. Bottcher, and M. S. Pindzola, *Phys. Rev. A* **25**, 154 (1982).

¹²S. E. Harris, D. J. Walker, R. G. Caro, A. J. Mendelsohn, and R. D. Cowan, *Opt. Lett.* **9**, 68 (1984).

¹³W. Lotz, *Z. Phys.* **220**, 466 (1969).